

EDOT-based conjugated polymers accessed via C–H direct arylation for efficient photocatalytic hydrogen production

Zhi-Rong Tan,^a Yu-Qin Xing,^a Jing-Zhao Cheng, Guang Zhang,^b Zhao-Qi Shen,^a Yu-Jie Zhang,^a Guangfu Liao,^c Long Chen,^b and Shi-Yong Liu^{*a}

^a College of Materials, Metallurgical and Chemistry, Jiangxi University of Science and Technology, Ganzhou 341000, P. R. China

^b Department of Chemistry, Tianjin University, Tianjin 300072, P. R. China

^c Engineering Research Center of Nano-Geomaterials of Ministry of Education, China University of Geosciences, Wuhan 430074, China

Corresponding author:

* E-mail: chelsy@zju.edu.cn, chelsy@jxust.edu.cn (S. -Y. Liu)

Characterizations

Fourier transformed infrared (FTIR) spectra were recorded on an FT-IR spectrometer (Bruker, ALPHA) using a standard KBr pellet technique in the frequency range of 4000–500 cm^{-1} . Solid state magic angle spinning ^{13}C CP/MAS NMR measurements were carried out on a Bruker Avance 400 model 400 MHz NMR spectrometer with a MAS rate of 10 kHz. Elemental analysis was measured by a Vario MICRO. The morphology of the photocatalysts was characterized by a scanning electron microscope (SEM, MLA650F, American). TEM images were obtained using a transmission electron microscope (TEM, Tecnai G2-20, American). The thickness of the photocatalysts was characterized by a Bruker Multimode 8 atomic force microscope (AFM) under Scan Asyst mode (Bruker, USA). Water contact angles were measured using JCY type measurement instrument (Shanghai Fang Rui Instrument Co. Ltd.). The UV–vis diffuse reflectance (DRS) spectra of the photocatalysts were recorded on UV-2600 scanning UV-vis spectrophotometer, using Ba_2SO_4 as the reference standard. Photoluminescence (PL) spectra was carried out on HORIBA Instruments FL-1000 fluorescence spectrometer. The DLS size distribution of the CPs was measured by a zetasizer (ZS90, Malvern Zetasizer Nano, UK). Pd content was determined by inductively coupled plasma optical emission spectrometer (Agilent ICP-OES 725). Transient photocurrent response (TPR) were measured by an electrochemical workstation (CHI650E/700E, Shanghai) equipped with a conventional three-electrode configuration using a platinum plate as the counter electrode and Ag/AgCl (saturated with KCl) as the reference electrode. To prepare the working electrodes, the photocatalyst was mixed with ethanol to form a slurry, then the above slurry was placed over an In-doped SnO_2 (ITO) glass (effective area of $1\text{ cm} \times 1\text{ cm}$), and a 0.1 M sodium sulfate aqueous solution was used as the electrolyte. Cyclic voltammetry (CV) measurement was carried out on a CHI660E (Chenhua, Shanghai) electrochemical workstation in a normal three electrode-cell system which using glassy carbon electrode as the working electrode, Ag/AgCl electrode as the reference electrode, platinum wire as the counter electrode. The tetra-n-butylammonium hexafluorophosphate (TBAPF_6 , 1.5 g) was used as a supporting electrolyte dissolved in 5 ml acetonitrile. According to the equation: $E_{\text{HOMO}} = -(E^{\text{OX}} + 4.8\text{ eV (v Ag/Ag}^+) - E^{\text{OX}}_{\text{Fc/Fc}^+})$, where $E^{\text{OX}}_{\text{Fc/Fc}^+}$ is the oxidation potential of ferrocene/ferrocenium (Fc/Fc⁺) couple, E_{HOMO} was calculated from the CV curves.

Apparent quantum yields measurements

The apparent quantum yield at different wavelengths was measured by inserting 400 nm, 450 nm, 500 nm, 550 nm, and 600 nm band-pass filters, and the irradiation was continued for 2 h for each wavelength region. The light intensity in the photocatalytic reaction was measured using a calibrated

power meter (Model 843R, Newport). The apparent quantum yields (AQY) was calculated according to the following equation:

$$AQY = \frac{\text{number of evolved } H_2 \text{ molecules} \times 2}{\text{number of incident photons}} \times 100\%$$

$$AQY = \frac{2M \times N_A \times h \times c}{S \times P \times t \times \lambda} \times 100\%$$

where M is the amount of H₂ molecules (mol); N_A is the Avogadro constant (6.022 × 10²³ mol⁻¹); h is the Planck constant (6.626 × 10⁻³⁴ J•s); c is vacuum light velocity (2.997 × 10⁸ m•s⁻¹); the irradiation area (S) is 25.5 cm² in our experiment; P is the intensity of the irradiating light (W•cm⁻²); t is the photoreaction time (s); and λ is the wavelength of the monochromatic light (m).

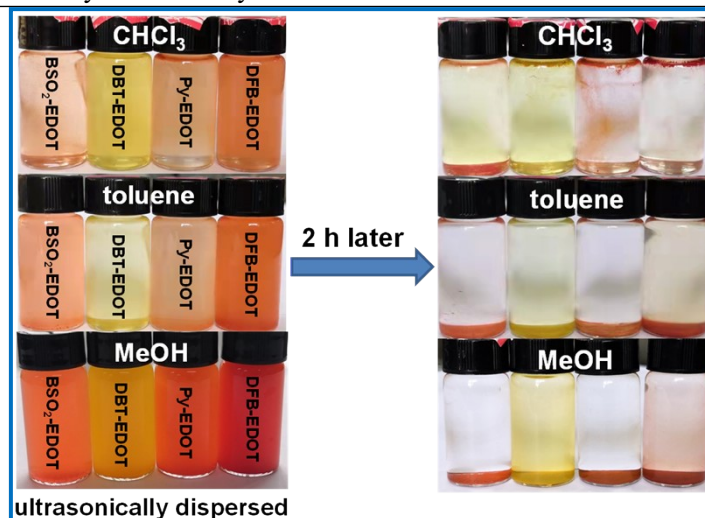


Fig. S1. Photograph of CPs dispersed in CHCl₃, toluene and MeOH *via* conventional sonication for 30 min, and then standing for 2 h.



Fig. S2 Photograph of CPs dispersed in NMP *via* conventional sonication for 30 min, and then standing for a week.

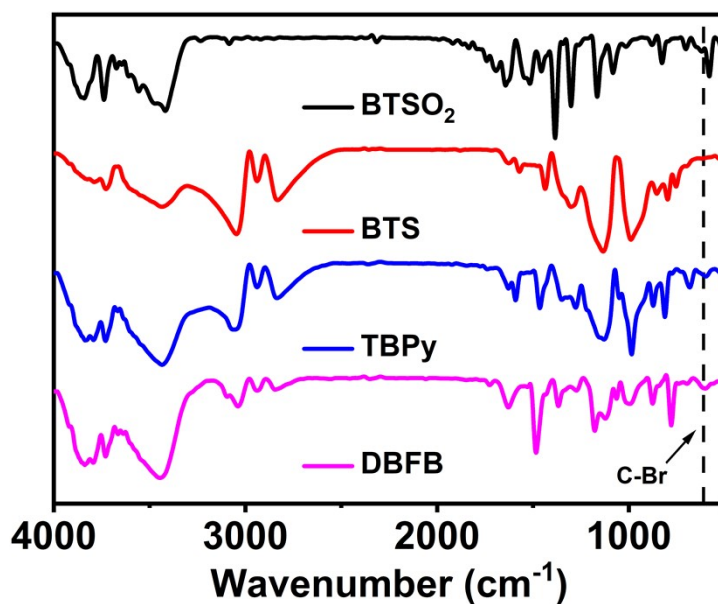


Fig. S3 FT-IR spectra of aryl bromides.

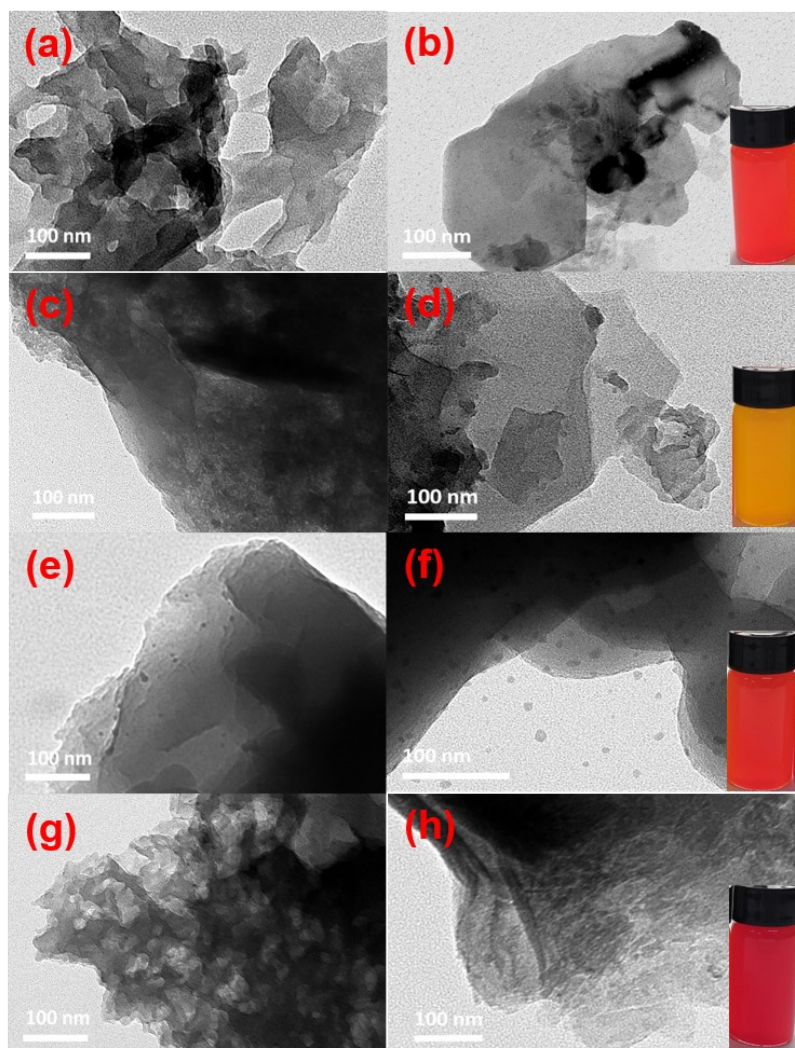


Fig. S4 TEM images of BSO₂-EDOT (a, b), DBT-EDOT (c, d), Py-EDOT (e, f), and DFB-EDOT (g, h) (insets: the photographs of CP colloidal dispersions in NMP). (The samples were ultrasonically dispersed in MeOH (a, c, e, g) and NMP (b, d, f, h), respectively, then dropped on the copper mesh).

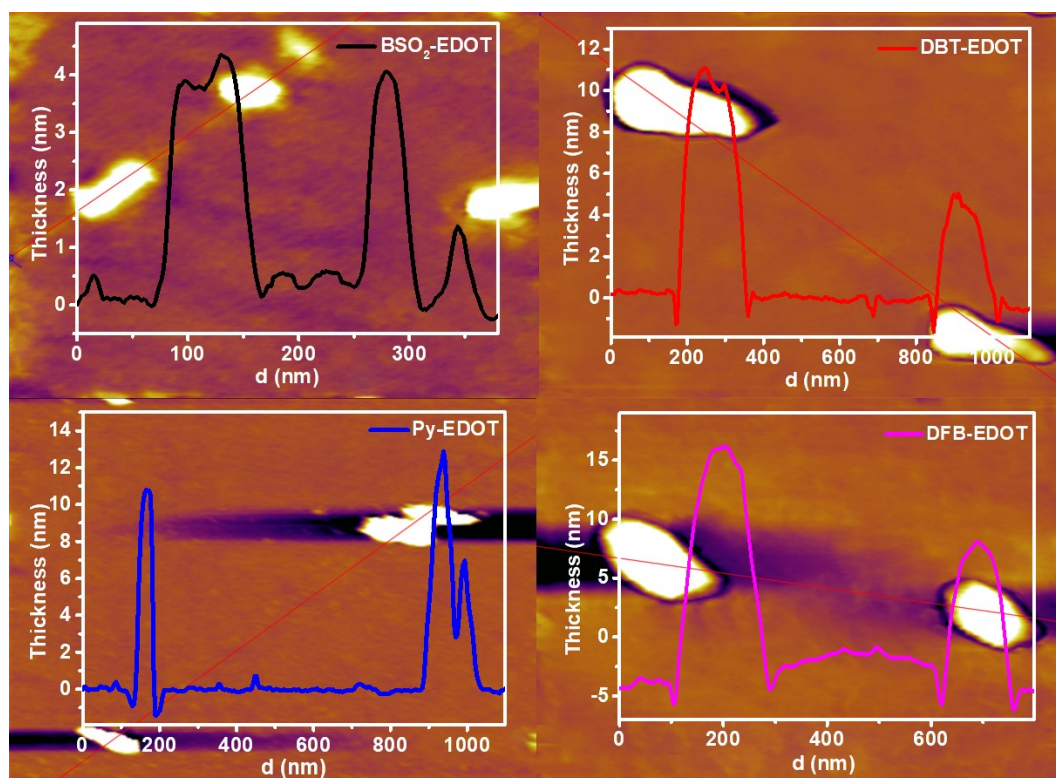


Fig. S5 AFM images and corresponding thickness analysis of the as-prepared CPs. (The samples were ultrasonically dispersed in NMP and then dropped on the mica slice).

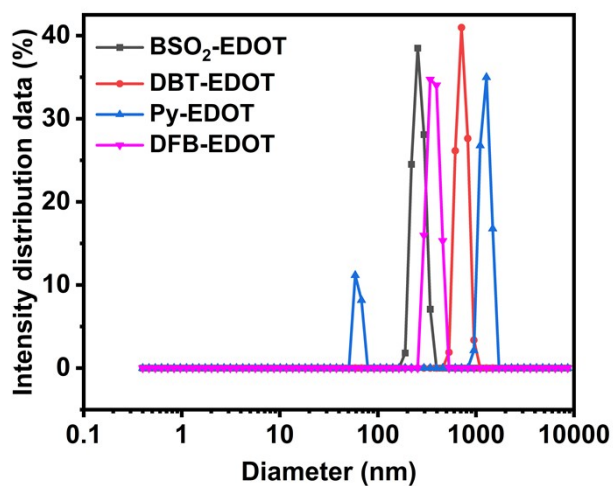


Fig. S6 Dynamic light scattering (DLS) size distributions of the CPs ultrasonically dispersed in NMP.

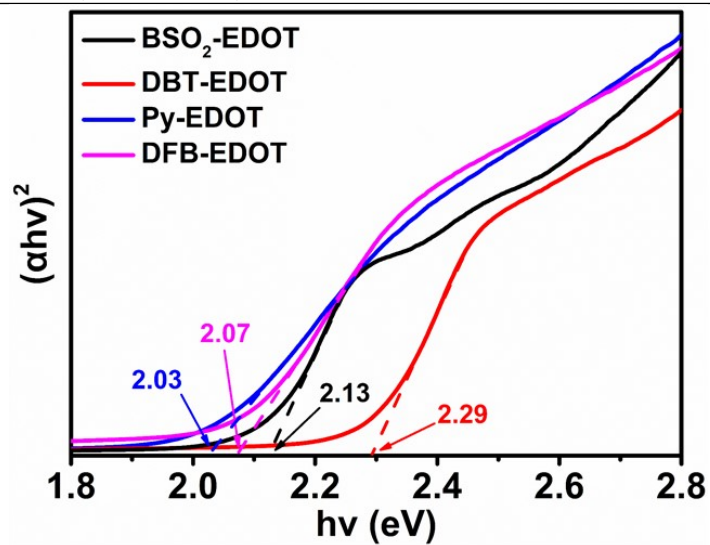


Fig. S7 Tauc plots of the transformed Kubelka–Munk function vs energy.

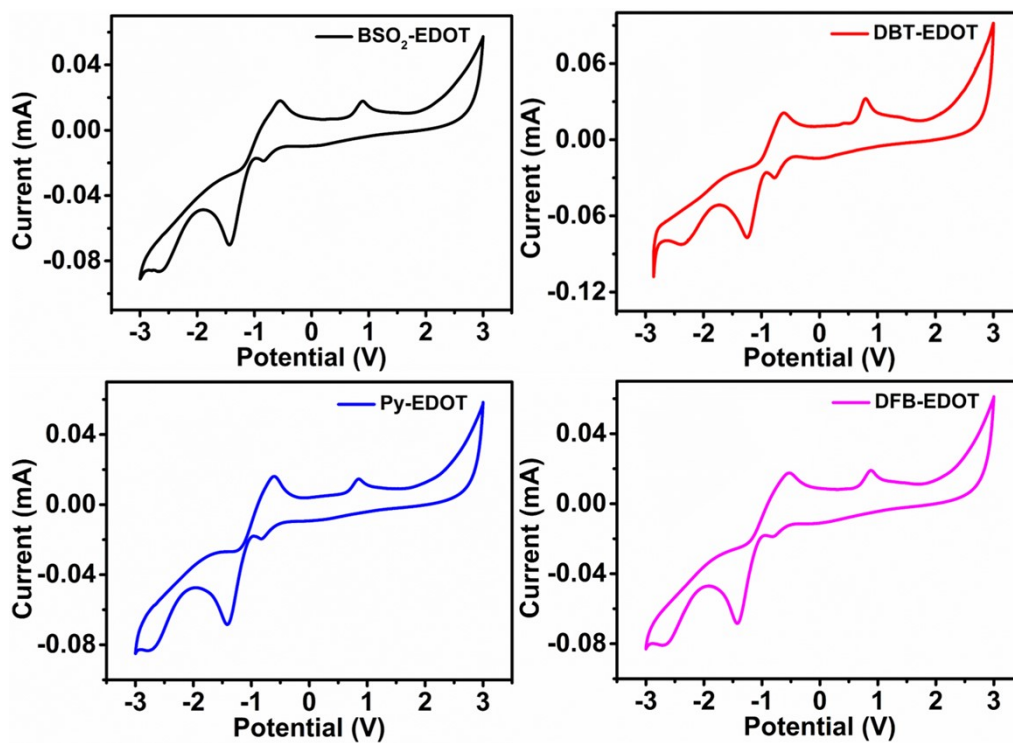
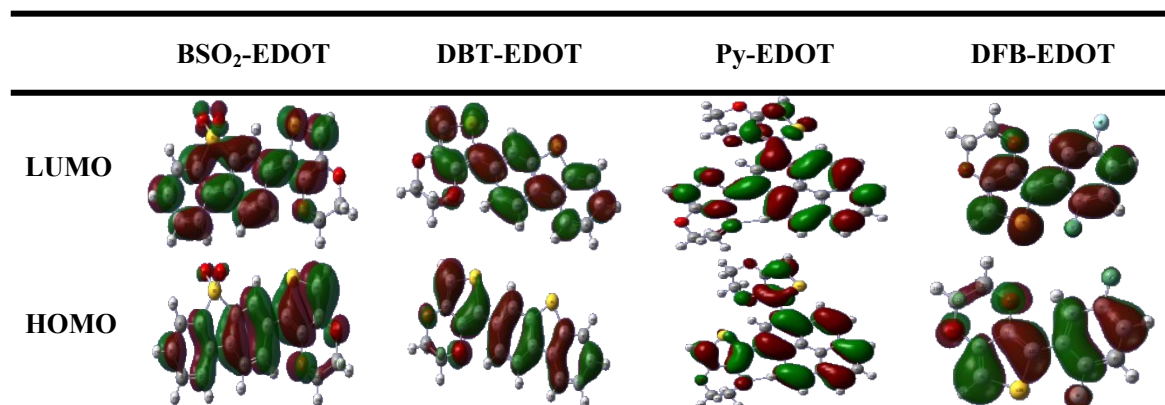


Fig. S8 CV curves of the as-prepared CPs.

Table S1 Distribution of frontier molecule orbitals (FMOs) of BSO₂-EDOT, DBT-EDOT, Py-EDOT, and DFB-EDOT predicted by DFT B3LYP/3-21+G**Table S2** Significant properties and HERs of 6 mg CPs photocatalysts in H₂O/NMP/AA.

CPs	E _g (eV)	LUMO (eV)	HOMO (eV)	HER (mmol h ⁻¹)
BSO ₂ -EDOT	2.13	-3.65	-5.78	0.95
DBT-EDOT	2.29	-3.35	-5.64	0.39
Py-EDOT	2.03	-3.58	-5.61	0.07
DFB-EDOT	2.07	-3.61	-5.68	0.13

Table S3 Summary of the PHP performances of organic photocatalysts.

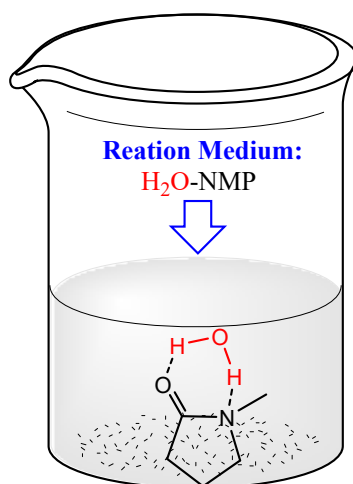
Photocatalyst	Synthetic methods	Co-catalyst	SED	λ (nm) ^f	HER(mmol h ⁻¹) (mass of photocatalyst)	AQY (%)	Ref.
BSO ₂ -EDOT ^a	DArP	--	AA	>420	0.95 (6 mg)	13.6@550 nm	This work
PTB7-Th:EH-IDTBR ^b (Linear CP)	Stille	Pt	AA	>350	0.13 (2 mg)	6.2@700 nm	1
PyBS-3 ^a	Suzuki	Pt	AA	>300	1.05 (10 mg)	29.3@420 nm	2
Py-CITP-BT-COF ^c	Schiff base	Pt	AA	>420	0.20 (20 mg)	8.45@420 nm	3
TtaTfa ^c	Schiff base	Pt	AA	>420	0.06 (3 mg)	1.43@450 nm	4
B-SOBT-1,3,5-E ^a	Sonogashira	--	TEOA	>420	0.28 (30 mg)	3.88@420 nm	5
NH ₂ -UiO-66/TpPa-1-COF ^d	--	Pt	SA	>420	0.23 (10 mg)	--	6
Cu-MIM ^d	--	--	TEA	>420	0.06 (1 mg)	--	7
CTF-BT/Th-1 ^e	--	Pt	TEOA	>420	0.33 (50 mg)	7.3@420 nm	8
BTT-CPP ^a	Suzuki	--	AA	>300	0.23 (6 mg)	3.3@365 nm	9
P10 ^a	Suzuki	--	TEA	>420	0.08 (25 mg)	11.6@420 nm	10
PFBT/CN ^a	Suzuki	Pt	TEOA	>420	0.07 (100 mg)	13.0@500 nm	11
P1 ^a	--	Pt	TEOA	>420	0.05 (50 mg)	3.58@420 nm	12
FS-COF ^c	Schiff base	Pt	AA	>420	0.05 (5 mg)	3.2@420 nm	13
N-PDBT-O ^a	Sonogashira	--	TEOA	>420	0.37 (30 mg)	3.7@420 nm	14
P-FSO ^a	Suzuki	--	TEOA	>420	0.40 (50 mg)	8.5@420 nm	15
DPP-bdy-TPA ^a	Suzuki	--	TEOA	>300	0.02 (3.5 mg)	9.6@420 nm	16
CP1 ^a	DArP	Pt	AA	>420	0.18 (6 mg)	4.62@550 nm	17

^a Conjugated polymers (CPs) or conjugated microporous polymer (CMP). ^b organic nanoparticles (NPs). ^c Covalent organic frameworks (COFs). ^d Metal-organic frameworks (MOFs)/covalent organic frameworks (COFs). ^e Covalent triazine frameworks (CTFs). AA: ascorbic acid, SA: sodium ascorbate, TEOA: triethanolamine, and TEA: trimethylamine. ^f All light sources are 300 W Xe lamp.

Table S4 HERs of PEDOT, BSO₂-EDOT and PBSO₂ for PHP under visible-light irradiation

Catalyst	Co-catalyst	SED	HER (mmol h ⁻¹ g ⁻¹)	Ref.
PEDOT	--	AA	none	This work
PBSO ₂	--	TEA	6.13	18
PBSO ₂	--	TEOA	2.46	19
PBSO ₂	--	TEA	3.26	10
BSO ₂ -EDOT	--	AA	158.4	This work

PEDOT **BSO₂-EDOT** **PBSO₂**

**Fig. S9** Schematic diagram for the hydrogen bond non-covalent interaction presented in NMP/H₂O mixed solvent as a medium for PHP reaction.

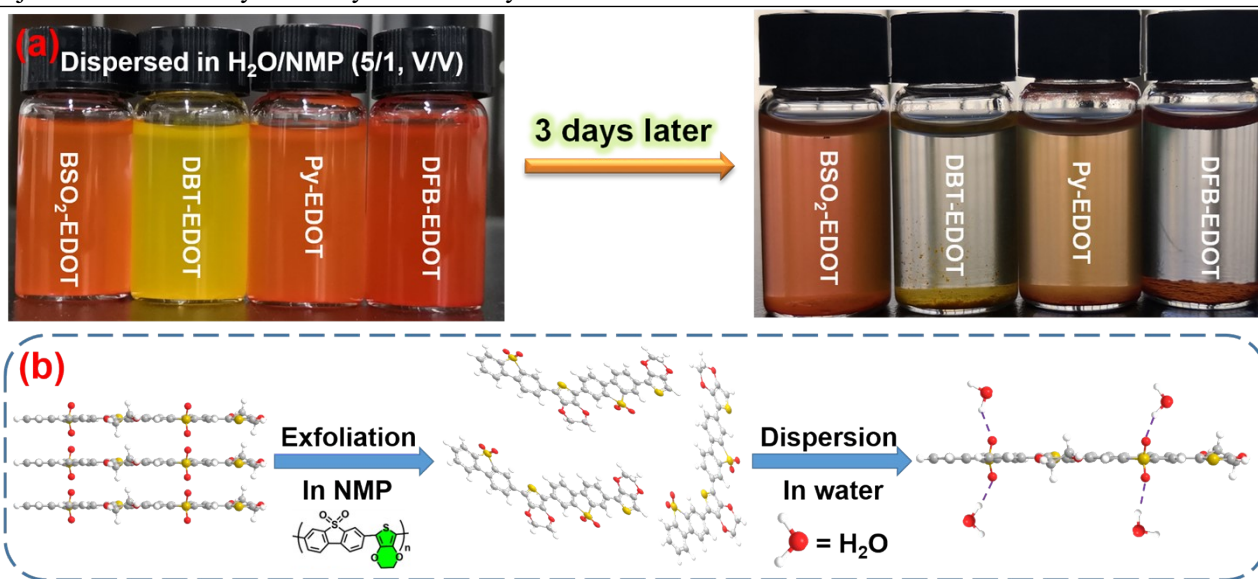


Fig. S10 (a) CPs ultrasonically dispersed in NMP aqueous solution, which were the same as those used for PHP tests (H₂O: NMP = 5:1). (b) Schematic diagram for the exfoliation of BSO₂-EDOT by NMP, and its colloidal dispersion in H₂O stabilized by hydrogen bonding [Grey balls: C; white balls: H; yellow balls: S; red balls: O.].

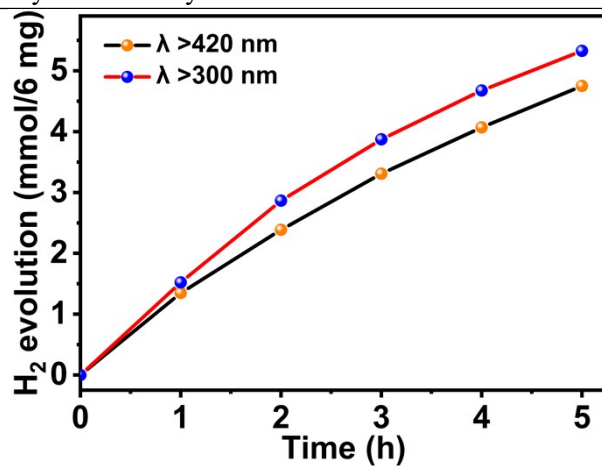


Fig. S11 HERs of BSO₂-EDOT under full-arc irradiation and visible light irradiation.

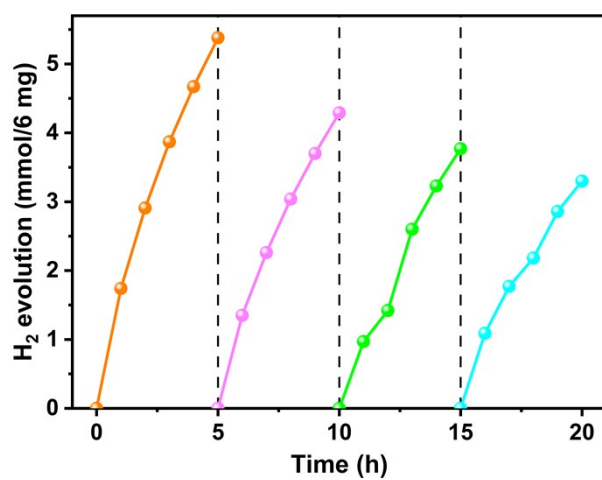
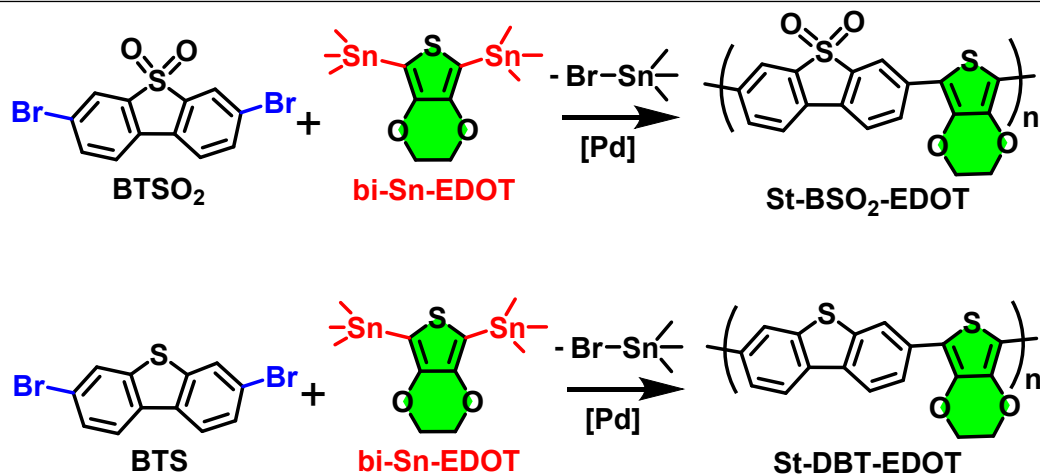


Fig. S12 Cycling test of PHP (evacuation every 5 h) for BSO₂-EDOT (6 mg).



Scheme S1 Synthetic routes for St-BSO₂-EDOT and St-DBT-EDOT via Stille coupling.

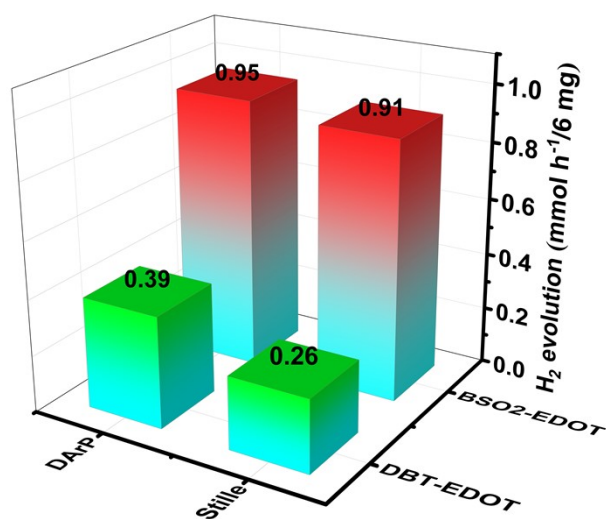
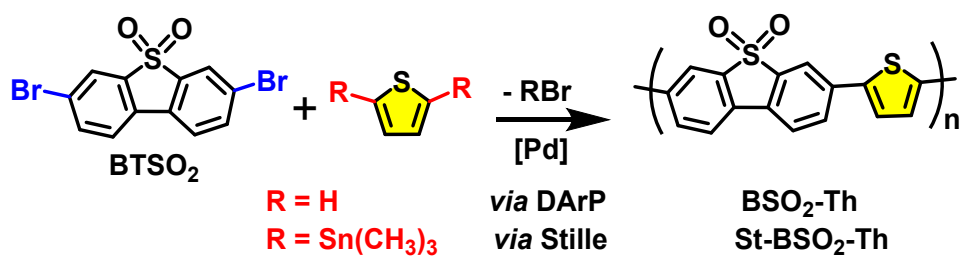


Fig. S13 HERs of BSO₂-EDOT, and DBT-EDOT synthesized via DArP or Stille coupling.



Scheme S2 Synthetic routes for BSO₂-Th and St-BSO₂-Th *via* DArP and Stille coupling, respectively.

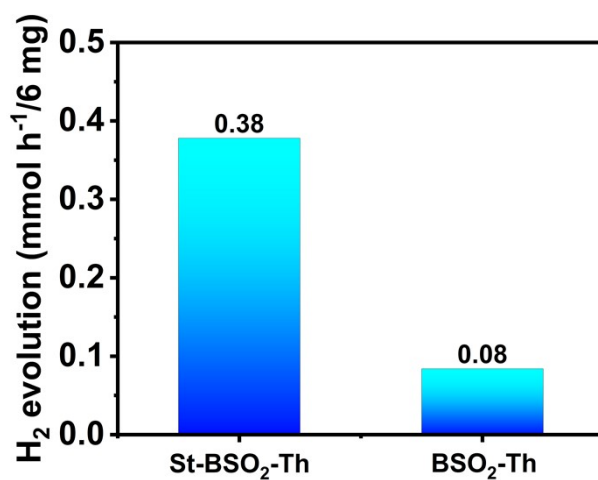


Fig. S14 HERs of BSO₂-Th and St-BSO₂-Th (6 mg) under visible light irradiation.

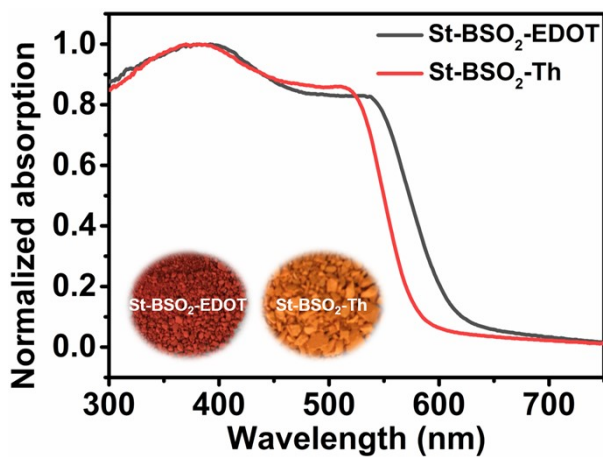


Fig. S15 UV-vis DRS spectra of St-BSO₂-EDOT and St-BSO₂-Th (inset: photographs of samples).

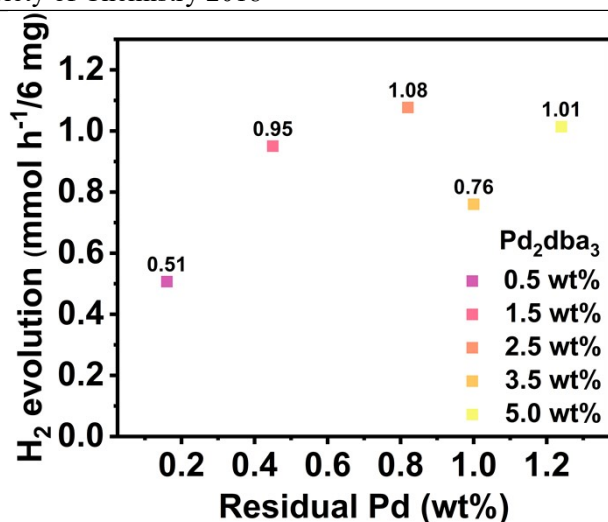


Fig. S16 Dependences of HERs on the amounts of residual Pd in BSO₂-EDOTs synthesized by different percentages of Pd₂dba₃. [The residual Pd are 0.16 wt%, 0.45 wt%, 0.82 wt%, 1.00 wt% and 1.24 wt%, respectively, for the BSO₂-EDOTs synthesized by 0.5%, 1.5%, 2.5%, 3.5% and 5.0% Pd₂dba₃.]

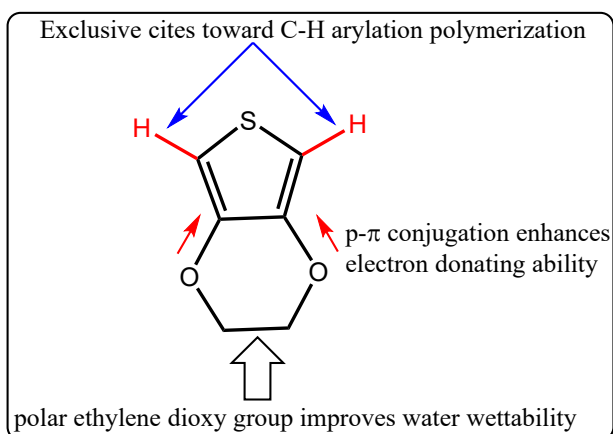


Fig. S17 Summarized merits of EDOT building block for CP-based photocatalysts.

References

- 1 J. Kosco, M. Bidwell, H. Cha, T. Martin, C. T. Howells, M. Sachs, D. H. Anjum, S. Gonzalez Lopez, L. Zou, A. Wadsworth, W. Zhang, L. Zhang, J. Tellam, R. Sougrat, F. Laquai, D. M. DeLongchamp, J. R. Durrant and I. McCulloch, *Nat. Mater.*, 2020, **19**, 559-565.
- 2 C. Shu, C. Han, X. Yang, C. Zhang, Y. Chen, S. Ren, F. Wang, F. Huang and J. X. Jiang, *Adv. Mater.*, 2021, **33**, 2008498.
- 3 W. Chen, L. Wang, D. Mo, F. He, Z. Wen, X. Wu, H. Xu and L. Chen, *Angew. Chem., Int. Ed.*, 2020, **59**, 16902-16909.
- 4 J. Yang, A. Acharjya, M. Y. Ye, J. Rabeah, S. Li, Z. Kochovski, S. Youk, J. Roeser, J. Gruneberg, M. Schwarze, T. Wang, Y. Lu, R. van de Krol, M. Oschatz, R. Schomacker, P. Saalfrank, A. Thomas and C. Penschke, *Angew. Chem., Int. Ed.*, 2021, DOI: 10.1002/anie.202104870.
- 5 X. Zhao, B. Chen, W. Dong, S. Wang, Y. Xiang and H. Chen, *J. Mater. Chem. A*, 2021, **9**, 10208-10216.
- 6 F.-M. Zhang, J.-L. Sheng, Z.-D. Yang, X.-J. Sun, H.-L. Tang, M. Lu, H. Dong, F.-C. Shen, J. Liu and Y.-Q. Lan, *Angew. Chem., Int. Ed.*, 2018, **57**, 12106-12110.
- 7 Y. Zang, J. Zhang, R. Wang, Z. D. Wang, Y. Zhu, X. Ren, S. Li, X. Y. Dong and S. Q. Zang, *Chem. Commun.*, 2020, **56**, 6261-6264.
- 8 W. Huang, Q. He, Y. Hu and Y. Li, *Angew. Chem., Int. Ed.*, 2019, **58**, 8676-8680.
- 9 J.-l. Wang, G. Ouyang, D. Wang, J. Li, J. Yao, W.-S. Li and H. Li, *Macromolecules*, 2021, **54**, 2661-2666.
- 10 M. Sachs, R. S. Sprick, D. Pearce, S. A. J. Hillman, A. Monti, A. A. Y. Guilbert, N. J. Brownbill, S. Dimitrov, X. Shi, F. Blanc, M. A. Zwijnenburg, J. Nelson, J. R. Durrant and A. I. Cooper, *Nat. Commun.*, 2018, **9**, 4968.
- 11 J. Chen, C. L. Dong, D. Zhao, Y. C. Huang, X. Wang, L. Samad, L. Dang, M. Shearer, S. Shen and L. Guo, *Adv. Mater.*, 2017, **29**, 1606198.
- 12 J. Yu, X. Sun, X. Xu, C. Zhang and X. He, *Appl. Catal., B*, 2019, **257**, 117935.
- 13 X. Wang, L. Chen, S. Y. Chong, M. A. Little, Y. Wu, W. H. Zhu, R. Clowes, Y. Yan, M. A. Zwijnenburg, R. S. Sprick and A. I. Cooper, *Nat. Chem.*, 2018, **10**, 1180-1189.
- 14 X. Wang, B. Chen, W. Dong, X. Zhang, Z. Li, Y. Xiang and H. Chen, *Macromol. Rapid Commun.*, 2019, **40**, 1800494.
- 15 Z. A. Lan, W. Ren, X. Chen, Y. F. Zhang and X. C. Wang, *Appl. Catal., B*, 2019, **245**, 596-603.
- 16 W. J. Xiao, Y. Wang, W. R. Wang, J. Li, J. D. Wang, Z. W. Xu, J. J. Li, J. H. Yao and W. S. Li, *Macromolecules*, 2020, **53**, 2454-2463.
- 17 W. Y. Huang, Z. Q. Shen, J. Z. Cheng, L. L. Liu, K. Yang, X. R. Chen, H. R. Wen and S. Y. Liu, *J. Mater. Chem. A*, 2019, **7**, 24222-24230.
- 18 Catherine M. Aitchison, R. S. Sprick and A. I. Cooper, *J. Mater. Chem. A*, 2019, **7**, 2490-2496.
- 19 G. Shu, Y. Li, Z. Wang, J.-X. Jiang and F. Wang, *Appl. Catal., B*, 2020, **261**, 118230.